#110

Papers from the GEOPHYSICAL LABORATORY
Carnegie Institution of Washington NO. 2042

High-temperature crystal chemistry of sodium zirconium phosphate (NZP)

R. M. Hazen and L. W. Finger
Geophysical Laboratory, Carnegie Institution of Washington, 2801 Upton Street, N. W., Washington, DC 20008

D. K. Agrawal and H. A. McKinstry
Materials Research Laboratory, The Pennsylvania State University, University Park, Pennsylvania 16802

Anthony J. Perrotta
Alcoa Technical Center, Alcoa Center, Pennsylvania 15069

(Received 18 July 1986; accepted 26 March 1987)

High-temperature crystal structures of NZP ($Na_{1+x}Zr_2P_{3-x}Si_xO_{12}$) have been determined by x-ray measurements made on single crystals. Thermal expansion of NZP ($x = 0.11$) parallel to the hexagonal c axis is positive (about $22.4\times10^{-6}\,°C^{-1}$ between 25° and 700 °C), whereas expansion perpendicular to c is slightly negative (about $5.4\times10^{-6}\,°C^{-1}$), resulting in an average volume thermal expansion of $11.8\times10^{-6}\,°C^{-1}$. A proposed structural model to interpret this anisotropic thermal expansion of NZP is tested to prove the model's validity. In this model the rotation of the phosphate tetrahedron is coupled to the rotation of the zirconium octahedron. The observed thermal expansions of sodium, zirconium, and phosphorus cation coordination polyhedra are 10.8, 0.00, and -0.23 (all $\times10^{-6}\,°C^{-1}$), respectively. The large thermal expansion of the sodium site is offset by rotations in the Zr–P polyhedral framework, thus yielding the low net expansion of NZP.

I. INTRODUCTION

The sodium zirconium phosphate $NaZr_2P_3O_{12}$ (NZP) structure, first determined 20 years ago by Hagman and Kierkegaard,[1] has several interesting features: (i) high ionic conductivity,[2] (ii) low thermal expansion,[3–5] and (iii) enormously varied ionic substitution in the structure.[6] The structural framework is such that a wide range of elements may be substituted at each of the different lattice positions (Li, Cs, Ca, Ba, etc., for Na; Ti, Ge, Hf for Zr, and Si, S for P). Sljukic *et al.*[7] observed that substitution of alkali for Na caused the cell parameters to change in an unusual way. Replacing Na with a large cation caused the c dimension of the rhombohedral cell to increase but anomalously the a dimension decreased. Alamo[8] noticed that the polyhedra are coupled and was able to postulate a model that could account for this anomaly. The details of this model have been described in the recent publication by Lenain *et al.*[9] The stability of this structure for a wide range of chemical elements makes this a candidate for a universal sponge for nuclear waste host material.[10] Boilot *et al.*[11] noticed that the thermal expansion behavior of $Na_{1+x}Zr_2P_{3-x}Si_xO_{12}$ (NASICON) was similarly anomalous.

Heating an alkali NZP material caused the c dimension to increase and the a dimension to decrease. Lenain *et al.*[12] examined all the alkali metal ions and found that Li had a positive expansion in both directions while K, Rb, Cs all behaved in a fashion similar to NZP. Limaye *et al.*[13] found that CaZP was similar but in Sr and Ba analogues the signs were reversed, i.e., the a axis expanded and the c axis contracted. Since all members of the family should, in principle, form crystalline solutions, a wide range of anisotropy and a near-zero thermal expansion composition should be possible.

The electrical properties of these materials are of considerable interest as well, since by replacing P with Si in NASICON, a material is produced that rivals β-Al_2O_3 as an ionic conductor[2] for industrial solid-state electrolyte applications in high-temperature batteries.

In the [NZP] structure the P ion is located on a horizontal twofold axis, and the tetrahedron is constrained to rotate about this axis. The Zr ion is located on a threefold axis, and the octahedron is therefore constrained to rotate about a vertical axis. Lenain *et al.*[9] have proposed that since the two different kinds of polyhedra are linked to each other at every corner, any rotation of the octahedron about the threefold vertical axis is accompanied by a similar rotation of the tetrahedron about the twofold horizontal axis. This linkage causes the cell dimensions to alter in response to the rotation of the polyhedra, due to thermal energy. The rotation of essentially rigid polyhedra also is accompanied by the changes in the environment and opening of the Na site, and consequently the conductivity path for the alkali ion is modified considerably. The model of Lenain *et al.*[9] does not explain the anomalous alteration of positive

 0003-6951/87/030329-09$01.75

and negative thermal expansion as found in $Ca_{1-x}Sr_xZr_4P_6O_{24}$. Further studies will be necessary to elucidate that.

Tran Qui *et al.*[14] have studied high-temperature structures of $Na_4Zr_2Si_3O_{12}$, which is the other end member of the $Na_{1+x}Zr_2P_{3-x}Si_xO_{12}$ system, and observed that with temperature little change occurred in bond distances and polyhedra angles in the $(Zr_2Si_3O_{12})^{-4}$ framework, whereas the Na–O polyhedra expand dramatically. Recently, Oota and Yamai[15] have studied the thermal expansion of NZP compounds at high temperature using powdered or sintered samples of the material. They reported that in the system $Na_{1+x}Zr_2P_{3-x}Si_xO_{12}$ the lattice parameter a decreases with temperatures up to $x = 1$ and then gradually increases while the c axis always increases faster with temperature for all x values.

Didisheim and Wuensch[16] reported the high-temperature structures of $Na_{1+x}Zr_2Si_xP_{3-x}O_{12}$ with $1.6 < x < 2.2$ based on neutron powder experiments. Their results agree with those of Oota and Yamai.[15] They reported that the anisotropic coefficients of thermal expansion for the composition $x = 2$ are 1.6×10^{-5} and $3.2 \times 10^{-6}\,°C^{-1}$, parallel to and normal to the c axis, respectively.

The principal objective of these high-temperature x-ray measurements on NZP is to determine the thermal expansion mechanisms of the phosphorus end member $NaZr_2P_3O_{12}$ and to compare these results with the predictions of Lenain *et al.*[9]

TABLE I. Unit-cell parameters, refinement conditions, and refined atomic positions.

		25 °C	270 °C	490 °C	690 °C
A (Å)		8.820 5(9)	8.809(1)	8.797(1)	8.7885(7)
C (Å)		22.769(1)	22.929(2)	23.017(2)	23.116(1)
V (Å^3)		1534.1(3)	1540.8(4)	1524.4(4)	1546.2(3)
Number of observations ($I > 2\sigma_I$)		201	211	202	206
R (%)[a]		0.9	1.4	1.4	1.7
WR (%)[b]		1.1	1.5	1.7	1.8
Extinction, r[c] ($\times 10^5$)		2.1(1)	1.8(2)	2.4(2)	2.3(2)
Na1	x	0	0	0	0
	y	0	0	0	0
	z	0	0	0	0
	B	3.72(5)	7.5(1)	11.6(5)	16.4(4)
Na2	Occupancy	0.017 1(10)	0.024(2)	0.029(2)	0.018(3)
	x	0.035(6)	0.037(7)	0.051(9)	0.048(11)
	y	0.335(10)	0.341(10)	0.354(11)	0.366(14)
	z	0.091(3)	0.096(2)	0.096(3)	0.088(6)
	B	0.2(8)	3.6(12)	6(2)	4(2)
Zr	x	0	0	0	0
	y	0	0	0	0
	z	0.145 72(1)	0.146 20(2)	0.146 61(2)	0.146 88(2)
	B	0.46(1)	0.76(2)	0.99(2)	1.30(2)
P	Occupancy of Si	0.037	0.037	0.037	0.037
	x	0.291 62(7)	0.290 73(10)	0.290 06(13)	0.289 39(12)
	y	0	0	0	0
	z	1/4	1/4	1/4	1/4
	B	0.60(3)	0.92(3)	1.18(4)	1.49(4)
O1	x	0.184 22(17)	0.181 89(24)	0.179 8(3)	0.178 1(4)
	y	−0.017 03(17)	−0.021 23(24)	−0.024 5(3)	−0.027 3(4)
	z	0.195 22(6)	0.195 73(8)	0.196 27(10)	0.196 53(11)
	B	1.42(3)	2.24(4)	2.79(6)	3.48(6)
O2	x	0.193 96(16)	0.195 20(22)	0.196 0(3)	0.196 7(3)
	y	0.170 67(17)	0.171 03(24)	0.171 2(3)	0.172 0(3)
	z	0.087 17(6)	0.088 51(8)	0.089 70(10)	0.090 54(11)
	B	1.10(3)	1.77(4)	2.27(5)	2.90(5)

[a] $R = \Sigma[|F_0| - |F_c|]/\Sigma F_0$.
[b] Weighted $R = [\Sigma w(|F_0| - |F_c|)^2/\bar{\Sigma} w F_0^2]^{1/2}$.
[c] Parenthesized figures represent e.s.d.'s.

II. EXPERIMENTAL

A. Specimen description

Crystals of synthetic $Na_{1+x}Zr_2Si_xP_{3-x}O_{12}$ with $x = 0.11$ were grown by the following technique. A mixture of Na_2CO_3, ZrO_2, and $NH_4H_2PO_4$ in molar ratio of 1:1:2 and small amount of SiO_2 were placed in a platinum crucible and fired at 170 °C for 4 h, at 900 °C for 4 h, at 1200 °C for 20 h, and finally at 1550 °C for 3 h—the heating rate throughout the schedule being maintained at 2°/min. After this the mixture was subjected to cooling at the rate of 5 °C/min to room temperature. The resultant material was washed in water to remove the excess sodium and phosphorus oxides. The silicon-to-phosphorus ratio was determined by electron microprobe analysis of the sample.

B. Data collection

An equant crystal of 100 μm diam was mounted in a silica glass capillary as described by Hazen and Finger.[17] A room-temperature study was performed on this crystal in the same configuration used in high-temperature experiments. A resistance heater of the type designed by Ohashi was employed to determine unit-cell parameters and x-ray intensity data on a four-circle diffractometer. Temperature was controlled and corrected for x-axis "chimney effects" by an automated feedback system.[18]

The unit-cell parameters at four temperatures (Table I) were determined from the position of 18 reflections between 39° and 43° 2θ. Each reflection was measured in four equivalent positions with $-90° \leqslant \chi \leqslant 90°$. Unit-cell parameters were first refined without symmetry constraints (i.e., as triclinic); all are consistent with hexagonal symmetry. Final reported unit-cell parameters were refined with hexagonal constraints.

Intensities were collected on an automated, four-circle diffractometer with Nb-filtered MoK_α radiation ($\lambda = 0.7093$ Å). All accessible reflections in one quadrant with $(\sin\theta)/\lambda < 0.7$ were collected at 298, 543, 763, and 963 K (all high temperatures $\pm$ 10 K). Omega step increments of 0.025° and 4 s/step counting times were employed. Digitized data were converted to graphical form and integrated peak intensities were determined by the method of Lehmann and Larsen[19] with an option for manual intervention. Corrections were made for Lorentz and polarization effects, as well as crystal absorption. For each temperature, intensities of symmetrically equivalent reflections were averaged to yield from 201 to 211 independent observed reflections (Table I). Conditions of refinement and final positional parameters are also given in Table I. Refined anisotropic temperature parameters and the magnitudes and orientation of thermal vibration ellipsoids at room conditions appear in Table II. Observed and calculated

TABLE IIA. Thermal vibration ellipsoids at 25 °C.

Atom	Parameter	$\beta \times 10^4$	Axis	rms (Å) displacement	Angle with respect to a	b	c
P	β_{11}	22(1)	r_1	0.078(2)	90	46(4)	126(4)
	$\beta_{22} = 2\beta_{12}$	26(1)	r_2	0.079(3)	180	60	90
	β_{33}	3.4(2)	r_3	0.101(2)	90	59(4)	36(4)
	$\beta_{13} = \frac{1}{2}\beta_{23}$	1.1(2)					
Zr	$\beta_{11} = \beta_{22} = 2\beta_{12}$	21(1)	r_{11}	0.077(2)	90	90	0
	β_{33}	1.9(1)	r_1	0.079(2)	150	90	90
	$\beta_{13} = \beta_{23} = 0$						
Na1	$\beta_{11} = \beta_{22} = 2\beta_{12}$	215(5)	r_{11}	0.122(5)	90	90	0
	β_{33}	5.6(5)	r_1	0.252(5)	120	120	90
	$\beta_{13} = \beta_{23} = 0$						
O1	β_{11}	57(3)	r_1	0.105(4)	38(3)	121(4)	53(3)
	β_{22}	64(3)	r_2	0.138(3)	101(6)	139(6)	88(6)
	β_{33}	7.3(3)	r_3	0.154(3)	54(3)	115(6)	143(3)
	β_{12}	34(2)					
	β_{13}	−5.2(7)					
	β_{23}	1.4(7)					
O2	β_{11}	38(3)	r_1	0.097(4)	57(5)	75(4)	124(80)
	β_{22}	49(3)	r_2	0.117(3)	117(3)	94(6)	145(8)
	β_{33}	4.7(3)	r_3	0.137(3)	135(5)	16(4)	85(5)
	β_{12}	13(2)					
	β_{13}	2.0(6)					
	β_{23}	2.1(6)					

TABLE IIB. Thermal vibration ellipsoids at 270 °C.

Atom	Parameter	$\beta \times 10^4$	Axis	rms (Å) displacement	Angle with respect to *a*	*b*	*c*
P	β_{11}	36(1)	r_1	0.093(2)	90	53(9)	136(3)
	$\beta_{22} = 2\beta_{12}$	43(2)	r_2	0.100(3)	180	60	90
	β_{33}	4.6(2)	r_3	0.127(2)	90	51(4)	46(3)
	$\beta_{13} = \frac{1}{2}\beta_{23}$	2.11(2)					
Zr	$\beta_{11} = \beta_{22} = 2\beta_{12}$	35(1)	r_{11}	0.090(2)	90	90	0
	β_{33}	3.1(1)	r_1	0.102(1)	150	90	90
	$\beta_{13} = \beta_{23} = 0$						
Na1	$\beta_{11} = \beta_{22} = 2\beta_{12}$	444(12)	r_{11}	0.146(7)	90	90	0
	β_{33}	8.1(8)	r_1	0.362(4)	120	120	90
	$\beta_{13} = \beta_{23} = 0$						
O1	β_{11}	92(4)	r_1	0.124(4)	41(3)	118(3)	50(2)
	β_{22}	108(4)	r_2	0.178(3)	101(6)	139(6)	86(7)
	β_{33}	111	r_3	0.195(3)	51(3)	118(7)	139(2)
	β_{12}	56(3)					
	β_{13}	−10(1)					
	β_{23}	2(1)					
O2	β_{11}	62(4)	r_1	0.111(5)	61(3)	74(3)	129(4)
	β_{22}	79(4)	r_2	0.155(3)	123(6)	92(7)	139(4)
	β_{33}	7.3(4)	r_3	0.175(3)	133(6)	16(3)	81(6)
	β_{12}	20(3)					
	β_{13}	5.8(9)					
	β_{23}	5.9(9)					

TABLE IIC. Thermal vibration ellipsoids at 490 °C.

Atom	Parameter	$\beta \times 10^4$	Axis	rms (Å) displacement	Angle with respect to *a*	*b*	*c*
P	β_{11}	43(2)	r_1	0.106	0	120	90
	$\beta_{22} = 2\beta_{12}$	54(3)	r_2	0.106	90	49	130
	β_{33}	6.6(3)	r_3	0.148	90	56	40
	$\beta_{13} = \frac{1}{2}\beta_{23}$	2.8(3)					
Zr	$\beta_{11} = \beta_{22} = 2\beta_{12}$	44(1)	r_{11}	0.109	90	90	0
	β_{33}	4.4(2)	r_1	0.112	150	90	90
	$\beta_{13} = \beta_{23} = 0$						
Na1	$\beta_{11} = \beta_{22} = 2\beta_{12}$	694(27)	r_{11}	0.187	90	90	0
	β_{33}	13(1)	r_1	0.449	90	150	90
	$\beta_{13} = \beta_{23} = 0$						
O1	β_{11}	122(6)	r_1	0.129(5)	45(3)	116(2)	46(2)
	β_{22}	147(6)	r_2	0.208(4)	97(20)	143(19)	91(20)
	β_{33}	12(1)	r_3	0.215(4)	46(6)	114(24)	136(3)
	β_{12}	79(4)					
	β_{13}	−13(1)					
	β_{23}	2(1)					
O2	β_{11}	65(5)	r_1	0.118(6)	50(3)	77(3)	116(3)
	β_{22}	94(5)	r_2	0.184(4)	101(12)	105(15)	153(5)
	β_{33}	11(1)	r_3	0.195(4)	138(5)	20(11)	98(14)
	β_{12}	17(4)					
	β_{13}	9(1)					
	β_{23}	6(1)					

TABLE IID. Thermal vibration ellipsoids at 690 °C.

Atom	Parameter	$\beta \times 10^4$	Axis	rms (Å) displacement	Angle with respect to a	b	c
P	β_{11}	56(2)	r_1	0.121(2)	90	52(3)	135(2)
	$\beta_{22} = 2\beta_{12}$	71(3)	r_2	0.123(3)	180	60	90
	β_{33}	7.7(3)	r_3	0.163(2)	90	52(3)	45(2)
	$\beta_{13} = \frac{1}{2}\beta_{23}$	3.4(3)					
Zr	$\beta_{11} = \beta_{22} = 2\beta_{12}$	59(1)	r_{11}	0.122(2)	90	90	0
	β_{33}	5.5(2)	r_1	0.131(1)	90	150	90
	$\beta_{13} = \beta_{23} = 0$						
Na1	$\beta_{11} = \beta_{22} = 2\beta_{12}$	983(35)	r_{11}	0.216(10)	90	90	0
	β_{33}	17(2)	r_1	0.537(6)	90	150	90
	$\beta_{13} = \beta_{23} = 0$						
O1	β_{11}	150(6)	r_1	0.143(5)	42(2)	118(2)	49(2)
	β_{22}	190(6)	r_2	0.234(4)	64(17)	142(20)	128(17)
	β_{33}	15(1)	r_3	0.239(4)	60(16)	66(27)	116(21)
	β_{12}	106(5)					
	β_{13}	−16(1)					
	β_{23}	2(1)					
O2	β_{11}	90(5)	r_1	0.132(5)	55(2)	73(2)	118(2)
	β_{22}	114(5)	r_2	0.211(4)	99(13)	109(15)	150(5)
	β_{33}	14(1)	r_3	0.221(4)	144(5)	26(11)	99(14)
	β_{12}	21(4)					
	β_{13}	12(1)					
	β_{23}	9(1)					

structure factors at four temperatures are available from the authors on request.

III. RESULTS

A. Room-temperature refinement

The NZP is rhombohedral and belongs to space group $\bar{R}3c$ ($Z = 6$). Refined atomic coordinates of $Na_{1+x}Zr_2P_{3-x}Si_xO_{12}$ ($x = 0.11$) are in close agreement with those of Hagman and Kierkegaard[1] and Hong[20] for end member $NaZr_2P_3O_{12}$. The four P–O bonds in the near-regular tetrahedron (point symmetry 2) range from 1.524–1.525 Å, with O–P–O angles deviating by no more than 1.5° from the ideal 109.5° tetrahedral angle (Table III). Our observed mean P–O bond length of 1.525 Å (for a sample with some Si in the tetrahedral position) is slightly longer than the 1.522 Å value of Hong.[20]

The zirconium octahedron (point symmetry 3) contains three Zr–O1 bonds of 2.041 Å and three Zr–O2 bonds of 2.094 Å (Table III). The adjacent O–Zr–O angles range from 84°–93° at room temperature, reflecting the moderate distortion of this cation polyhedron. The observed polyhedral distortions (Table IV) justify the assumption in the angular distortion model of Lenain *et al.*[9] that ZrO_6 octahedra are more distorted than PO_4 tetrahedra.

The sodium Na1 site (point symmetry 3) is a very distorted octahedron, elongated parallel to the c axis. Six symmetrically equivalent Na–O2 bonds are 2.556 Å long; six adjacent O2–Na1–O2 angles are 66° and six are 114°, compared to the ideal 90° values of a regular octahedron.

The small excess of sodium (0.11 atoms per formula unit) is located in the Na2 site, which is a poorly constrained, irregular site at a general position. This site has five Na2–O bonds of about 2.4–2.6 Å and five additional Na2–O distances from 2.9–3.2 Å. Note that the Na2 site is fully occupied in the phosphorus-free end member $Na_4Zr_2Si_3O_{12}$.

The O1 oxygen is coordinated to one P and one Zr with a P–O1–Zr angle of about 157°. The O2 is three coordinated to one each of P, Zr, and Na1. The four atoms in the O2 cluster are almost coplanar.

Thermal vibration ellipsoids of NZP atoms (Table IIA) reveal significant vibration anisotropies for Na1 and the two oxygen atoms. The Na1 vibration may be described by a flattened ellipsoid with rms displacements parallel to c, only half of those in the (001) plane.

TABLE III. Selected bond distances and angles.

Bond/Angle		25 °C	270 °C	490 °C	690 °C
P tetrahedron					
P–O1	[2][a]	1.528(1)[b]	1.524(2)	1.519(2)	1.519(3)
P–O2	[2]	1.525(1)	1.522(2)	1.521(2)	1.519(2)
Mean P–O		1.525	1.522	1.520	1.519
O1–O1		2.503(2)	2.507(4)	2.501(5)	2.507(5)
O1–O2	[2]	2.465(2)	2.459(3)	2.457(3)	2.454(4)
O1–O2	[2]	2.507(2)	2.502(3)	2.495(3)	2.494(3)
O2–O2		2.490(3)	2.487(4)	2.488(5)	2.478(5)
O1–P–O1		110.3(1)	110.8(2)	110.8(2)	111.2(2)
O1–P–O2	[2]	107.9(1)	107.7(1)	107.8(1)	107.8(1)
O1–P–O2	[2]	110.6(1)	110.5(1)	110.3(1)	110.4(1)
O2–P–O2		109.5(1)	109.6(2)	109.7(2)	109.4(2)
Zr octahedron					
Zr–O1		2.044(1)	2.047(2)	2.048(2)	2.048(2)
Zr–O2		2.096(1)	2.093(2)	2.088(2)	2.087(2)
Mean Zr–O		2.067	2.070	2.068	2.068
O1–O1	[3]	2.951(2)	2.950(3)	2.944(4)	2.942(4)
O1–O2	[3]	2.937 (2)	2.952(3)	2.958(4)	2.968(4)
O1–O2	[3]	2.991(2)	2.982(3)	2.968(4)	2.957(4)
O2–O2	[3]	2.800(3)	2.811(3)	2.816(4)	2.825(4)
O1–Zr–O1	[3]	92.6(1)	92.2(1)	91.9(1)	91.7(1)
O1–Zr–O2	[3]	90.5(1)	91.0(1)	91.3(1)	91.2(1)
O1–Zr–O2	[3]	92.7(1)	92.2(1)	91.7(1)	91.7(1)
O2–Zr–O2	[3]	83.9(1)	84.4(1)	84.9(1)	85.2(1)
Na1 octahedron					
Na1–O2	[6]	2.556(1)	2.597(2)	2.629(2)	2.653(2)
O2–O2	[6]	2.800(2)	2.811(3)	2.816(4)	2.825(4)
O2–O2	[6]	4.287(3)	4.137(4)	4.440(6)	4.492(6)
O2–Na1–O2	[6]	66.4(1)	65.5(1)	64.8(1)	64.3(1)
O2–Na1–O2	[6]	113.6(1)	114.5(1)	115.2(1)	115.7(1)
O1 coordination					
O1–P		1.525(1)	1.523(2)	1.519(2)	1.519(2)
O1–Zr		2.041(1)	2.047(2)	2.048(2)	2.050(2)
Zr–O1–P		156.9(1)	156.2(1)	155.7(2)	155.0(2)
O2 coordination					
O2–P		1.524(1)	1.522(2)	1.521(2)	1.519(2)
O2–Zr		2.094(1)	2.093(2)	2.087(2)	2.087(2)
O2–Na1		2.556(1)	2.597(2)	2.629(2)	2.653(2)
P–O2–Zr		143.8(1)	145.3(1)	146.7(2)	147.7(2)
P–O2–Na1		126.0(1)	124.2(1)	122.6(1)	121.6(1)
Zr–O2–Na1		90.2(1)	90.5(1)	90.6(1)	90.7(1)

[a] Bracketed figures represent bond or angle multiplicities.
[b] Parenthesized figures represent e.s.d.'s.

TABLE IV. Polyhedral volumes and distortion indices.

	Atom	25 °C	270 °C	490 °C	690 °C
P	Vol (Å^3)	1.824(1)	1.812(3)	1.802(4)	1.796(5)
	QE[a]	1.000(2)	1.001(2)	1.000(2)	1.001(3)
	AV[b]	1.93	2.22	1.97	2.32
Zr	Vol (Å^3)	11.76(1)	11.78(1)	11.74(2)	11.76(2)
	QE	1.0041(5)	1.0034(7)	1.0027(8)	1.0024(10)
	AV	14.1	11.6	9.5	8.3
Na1	Vol (Å^3)	18.00(1)	18.53(2)	18.92(3)	19.29(4)
	QE	1.1566(4)	1.1685(5)	1.1793(6)	1.1859(7)
	AV	610	655	694	719

[a] QE = Quadratic elongation = $\Sigma_{i=1}^{n}[(l_i/l_0)^2/n]$.
[b] AV = Angle variance = $\Sigma_{i=1}^{n}[(\theta_i - \theta_0)^2/(n-1)]$.

The O1 oxygen (coordinated to one P and one Zr) has maximum vibrations in the plane perpendicular to the P–O1–Zr axis, whereas the O2 oxygen has maximum vibration in the direction perpendicular to the plane containing the P–O2, Zr–O2, and Na1–O2 bonds.

B. Thermal expansion

Unit-cell parameters at four temperatures (Table I) are in close agreement with the linear thermal expansion and temperature-volume data of Oota and Yamai.[15] The *c* axis undergoes an average positive expansion of 22.4×10^{-6} °C^{-1} between 25° and 690 °C, whereas the *a* axes contract by about 5.4×10^{-6} °C^{-1} over the same temperature range. The net volume expansion is about 11.8×10^{-6} °C^{-1}.

C. High-temperature crystal structure of NZP

In spite of the small thermal expansion of NZP, there are several significant changes in the sizes and orientations of structural elements, with changing temperature. The largest change in cation–anion distances occurs in the sodium site; Na1–O2 bonds expand from 2.556 Å at room temperature to 2.653 Å at 690 °C, corresponding to a linear bond expansion of 5.7×10^{-5} °C^{-1}. This value is comparable to Na–O expansion in alkali feldspars[21,22] and the zeolite natrolite[23] and in agreement with the data of Tran Qui *et al.*[14] on $Na_4Zr_2Si_3O_{12}$. In contrast, the Zr–O distance does not change with temperature, and the P–O distance *appears* to decrease from 1.525 to 1.519 Å over this temperature range. The actual expansion of Zr–O and P–O bonds may be slightly positive if corrections for correlated vibrational motion are taken into account.[24]

Changes in cation–anion–cation angles are particularly dramatic in NZP and are important in understanding the mechanisms of near-zero net thermal expansion in a compound with a rapidly expanding sodium site. All three P–O–cation angles (P–O1–Zr, P–O2–Zr, and P–O2–Na1) vary rapidly with increasing temperature.

IV. DISCUSSION

The rotation of the polyhedra of the structure can be described with reference to the angles defined in the structure model paper of Lenain *et al.*[9] In Fig. 1 the projections of ZrO_6 octahedron and PO_4 tetrahedron are shown; the angles of rotation θ and φ have also been defined. In Zr octahedron the plane formed by the three

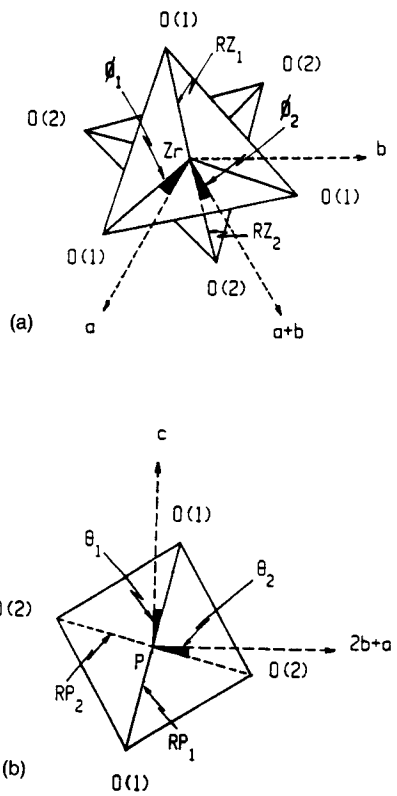

FIG. 1. (a) Projection of a ZrO_6 octahedron in the plane perpendicular to the threefold axis (*c* axis). (b) Projection of a PO_4 tetrahedron in the plane perpendicular to the twofold axis (*a* axis).

TABLE V. Rotations of polyhedra of [NZP] structure.

	Bond distances				Tetrahedron			Octahedron		
Temp.	P–O1	P–O2	Zr–O1	Zr–O2	θ_1	θ_2	$(\theta_2-\theta_1)$	ϕ_1	ϕ_2	$(\phi_2-\phi_1)$
25	1.528	1.525	2.044	2.096	− 6.0	− 4.0	1.9	− 4.4	− 6.31	− 2.4
270	1.524	1.522	2.047	2.094	− 7.4	− 5.5	1.9	− 5.4	− 6.52	− 1.9
490	1.519	1.521	2.048	2.088	− 8.6	− 6.8	1.8	− 6.2	− 6.67	− 1.7
690	1.519	1.519	2.049	2.087	− 9.5	− 7.7	1.8	− 6.9	− 6.62	− 1.3

O(1) will rotate faster than the O(2) plane, causing the angle O(1)–Zr–O(2) not to be equal to 60 degrees (shearing action). In P tetrahedron, the line O(1)–P–O(1) will rotate faster than the line O(2)–P–O(2), causing the angle between them to be different from 90 degrees.

The zero rotation position for the O1 oxygen is chosen when the y coordinate is zero. In the room-temperature structure, this atom has a y coordinate of − 0.017 03, which corresponds to a negative rotation of − 6.0 degrees (see Table V). This position leads to a rotation of the zirconium octahedron of − 4.4 degrees. The calculated values for these rotations are presented in Table V. The rotation continues in the negative sense as the temperature increases. The angular distortion of the polyhedra decreases with increasing temperature. Thus it has been demonstrated that the anomalous thermal expansion behavior of NZP structure is correlated with rotations of polyhedra in the Zr–P framework. A part of the unit cell of NZP lattice at 25° and 690 °C has been generated by a computer program based on the data listed in Table III; this has been shown in Fig. 2. A careful examination of these diagrams reveals that there is a slight change in the angles of rotation of two polyhedra at 690 °C.

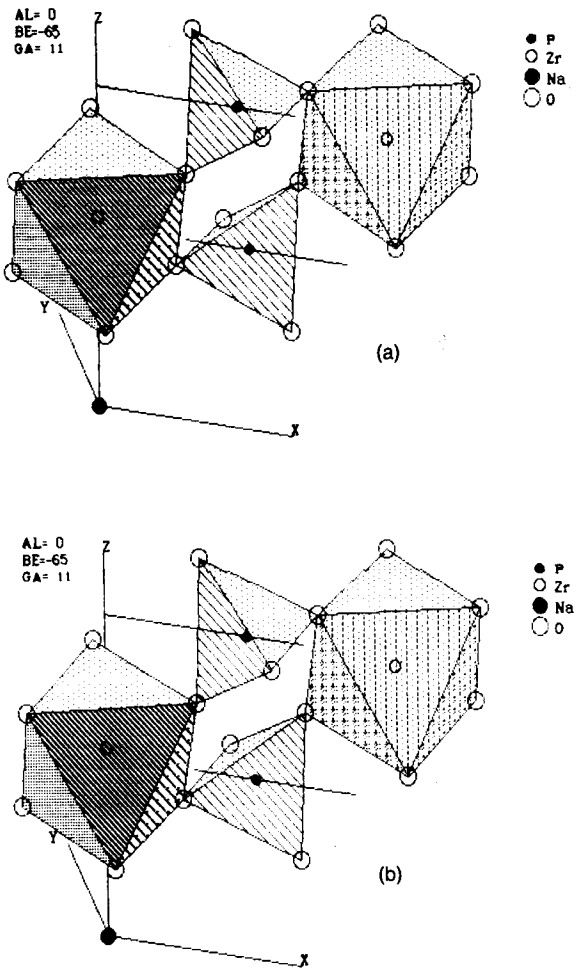

FIG. 2. Part of the NZP unit cell at (a) 25 °C, (b) 690 °C.

Most low thermal expansion materials are also characterized by unusually low compressibility; the same rigid structural elements that restrict expansion in zircon and silica glass, for example, also restrict compression. Materials with the NZP structure, however, may depart from this intuitively reasonable trend. Hazen and Finger[17] described bond compression and bond angle bending as two important compression mechanisms in ceramic-type materials. The NZP-type compounds have the potential for cooperative interaction of these two mechanisms, which could lead to large compressibilities ($> 10^{-4}$ kbar^{-1}). The expected structural distortions of rhombohedral NZP, furthermore, could lead to a high-pressure phase transition to the monoclinic form exhibited by intermediate members of the $Na_{1+x}Zr_2Si_xP_{3-x}O_{12}$ series.[11] High-pressure investigation of NZP is now in preparation to test these predictions.

ACKNOWLEDGMENTS

This research was supported by the National Science Foundation Grants No. EAR83-19209 and EAR84-19982, and United States Air Force Contract No. AFOSR 83-0291.

REFERENCES

[1]L. O. Hagman and P. Kierkegaard, Acta Chem. Scand. **22**, 1822 (1968).

[2]J. B. Goodenough, H. Y.-P. Hong, and J. A. Kafalas, Mater. Res. Bull. **11**, 203 (1976).

[3]J. Alamo and R. Roy, Am. Ceram. Soc. **67**, C78 (1984).

[4]R. Roy, D. K. Agrawal, J. Alamo, and R. A. Roy, Mater. Res. Bull. **19**, 471 (1984).

[5]D. K. Agrawal and V. S. Stubican, Mater. Res. Bull. **20**, 99 (1985).

[6]J. Alamo and R. Roy, J. Mater. Sci. **21**, 444 (1986).

[7]M. Sljukic, B. Matkovic, B. Prodic, and S. Scarnicar, Croatica Chemica Acta **39**, 145 (1967).

[8]J. Alamo (private communication).

[9]G. E. Lenain, H. A. McKinstry, J. Alamo, and D. K. Agrawal, J. Mater. Sci. **22**, 17 (1987).

[10]R. Roy, E. R. Vance, and J. Alamo, Mater. Res. Bull. **17**, 585 (1982).

[11]J. P. Boilot, J. P. Salanie, G. Desplaches, and D. LePotier, Mater. Res. Bull. **14**, 1469 (1969).

[12]G. E. Lenain, H. A. McKinstry, S. Limaye, and A. Woodword, Mater. Res. Bull. **19**, 1451 (1984).

[13]S. Y. Limaye, D. K. Agrawal, and H. A. McKinstry, J. Am. Ceram. Soc. (to be published).

[14]D. Tran Qui, J. J. Capponi, J. C. Joubert, and R. D. Shannon, J. Solid State Chem. **39**, 219 (1981).

[15]T. Oota and I. Yamai, J. Am. Ceram. Soc. **69**, 1 (1986).

[16]J. J. Didisheim and B. J. Wuensch, in *NBS Reactor, Summary of Activities July 1984 through June 1985, Washington*, NBS Technical Note 1217, edited by F. J. Shorten (United States Department of Commerce, Washington, DC, 1985), pp. 4–9.

[17]R. M. Hazen and L. W. Finger, *Comparative Crystal Chemistry* (Wiley, New York, 1982).

[18]L. W. Finger and H. E. King, Am. Mineral. **63**, 337 (1978).

[19]M. S. Lehmann and F. K. Larsen, Acta Crystallogr. A **30**, 580 (1974).

[20]H. Y.-P. Hong, Mater. Res. Bull. **11**, 173 (1976).

[21]C. T. Prewitt, S. Sueno, and J. J. Papika, Am. Mineral. **61**, 1213 (1976).

[22]J. K. Winter, F. P. Okamura, and S. Ghose, Am. Mineral. **64**, 409 (1981).

[23]D. R. Peacor, Am. Mineral. **58**, 676 (1973).

[24]W. R. Busing and H. A. Levy, Acta Crystallogr. **17**, 142 (1964).